American Mineralogist, Volume 78, pages 1096–1103, 1993

Fangite, Tl_3AsS_4, a new thallium arsenic sulfosalt from the Mercur Au deposit, Utah, and revised optical data for gillulyite

JAMES R. WILSON
Department of Geology, Weber State University, Ogden, Utah 84408, U.S.A.
PRADIP K. SEN GUPTA†
Department of Geology, Memphis State University, Memphis, Tennessee 38152, U.S.A.
PAUL D. ROBINSON
Department of Geology, Southern Illinois University, Carbondale, Illinois 62901, U.S.A.
ALAN J. CRIDDLE
The Natural History Museum, Cromwell Road, London SW7 5BD, England

ABSTRACT

Fangite, Tl_3AsS_4, is one of several Tl minerals that occur at the Mercur disseminated Au deposit, Tooele County, Utah. The mineral is described on the basis of one specimen found in a sulfide ore stockpile at the mine. It occurs in a vug with pyrite and other sulfide material of complex composition. Realgar and orpiment occur in calcite veins in the host rock, but not in the vug.

Fangite has a deep red to maroon color and an orange streak. It is translucent but tarnishes to a nearly metallic luster. The calculated density is 6.185 g/cm³, and the measured density (determined from synthetic Tl_3AsS_4) is 6.20(4) g/cm³. The Mohs hardness is 2.0–2.5, and the mean VHN_{100} is 60.7. Fangite is blue-gray in polished section and has very low bireflectance, with a difference in Y% of 0.4. Red internal reflections are abundant. Reflectivity values in air range from 21.1 to 30.15%; immersion values range from 8.08 to 14.7%.

A single-crystal X-ray diffraction study shows fangite to be orthorhombic, space group *Pnma*, with unit-cell parameters a = 8.894(8), b = 10.855(9), c = 9.079(9) Å, V = 877(1) Å³, and Z = 4. The structure was solved by direct methods and refined to a final residual of 0.046 using 637 observed reflections. The As atom is in tetrahedral coordination with S, whereas the Tl2 atom is in fivefold coordination with S, producing trigonal dipyramids. The dipyramids and tetrahedra are interconnected to form polyhedral layers parallel to (010). Interlayer Tl1 atoms link the layers.

Because of problems with internal reflections in the original published data, new optical data for gillulyite (another Tl mineral from this deposit) are presented. Gillulyite, $Tl_2(As,Sb)_8S_{13}$, is distinctively bireflectant, with a difference in Y% of 3.8%. Reflectivity values in air range from 21.2 to 32.0%; immersion values range from 8.14 to 18.6%.

INTRODUCTION

Fangite, Tl_3AsS_4, is a thallium arsenic sulfosalt that occurs at the Mercur Au deposit in the southern Oquirrh Mountains, Tooele County, Utah, approximately 56 km southwest of Salt Lake City. The Mercur deposit is a sediment-hosted, disseminated Au deposit that is characterized by micrometer-sized native gold and a Tl-As-Hg-Sb geochemical signature. The general geology of the Mercur area was described by Gilluly (1932). Previous studies pertaining to the geological and geochemical characteristics of the Mercur Au deposit include those of Jewell and Parry (1987, 1988), Kornze (1987), Tafuri (1987), Stanger (1992), Kroko and Bruhn (1992), and Wilson and Parry (1990a, 1990b, 1992). Recent descriptions of the mineral assemblage of the deposit can be found in Wilson et al. (1991), and Wilson and Wilson (1991, 1992).

The specimen used in the microprobe study and the synthetic material described in this article have been deposited in the National Museum of Natural History, Smithsonian Institution (fangite, NMNH 17071; synthetic material, NMNH 17072). No other specimens are available. The mineral is named for Jen-Ho Fang, currently at the University of Alabama, for his numerous contributions to the fields of crystallography, crystal chemistry, and geostatistics. The mineral description and name were approved by the International Mineralogical

†Deceased August, 1992.

0003–004X/93/0910–1096$02.00

Association Commission on New Minerals and Mineral Names.

Material compositionally identical to fangite was identified by El Goresy and Pavicevic (1988) from the Crven Dol deposit in Alshar, Former Yugoslavian Republic of Macedonia. In this occurrence it was found as thin rims (<2 mm) on lorandite, orpiment, and realgar. Engel and Nowacki (1984) determined the structure of synthetic Tl_3AsS_4; however, their published work lacks crystal structure detail. In this paper we describe the physical, chemical, and crystallographic properties of fangite, including a redetermination and detailed description of the structure.

Occurrence

Fangite was found in one boulder from a sulfide stockpile at the 6080 level in the brickyard cut of the Marion Hill pit at the Mercur Au deposit. Most of this pit has been excavated in oxidized ore, and only a few pods of sulfide ore were encountered. The specimen occurred in a small vug within a silty, C-rich limestone boulder derived from the Mercur mine series of the Mississippian Great Blue Limestone. Calcite veins in the boulder contained realgar and orpiment.

Fangite is associated with subhedral pyrite (20–40 mm) and fine-grained sulfide material (2–20 mm) of complex chemical composition that occurs in brecciated(?) veinlets extending from the vug. This fine-grained material most probably represents partial replacement of pyrite, sphalerite, or other sulfides. Electron microprobe analyses indicate that some grains are probably As- and Tl-rich pyrite, others are As-, Fe-, and Tl-bearing sphalerite, and some are complex mixtures of arsenic, iron, zinc, and thallium sulfides. All of these fine-grained sulfides have Sb as a minor constituent in the 0.9–1.8% range. In polished section, fangite occurs as irregular grains with occasional subhedral outlines. Representative grains measure 0.9 × 0.5 mm and 0.4 × 0.4 mm.

The single occurrence of fangite in an isolated vug precludes any definitive statement about its origin and relationships with the other thallium sulfosalts, and with the realgar and orpiment that occur in this deposit. However, based on the nature of the accompanying material, as well as the observations of El Goresy and Pavicevic (1988), it is reasonable to postulate that fangite forms as an alteration product of earlier thallium sulfosalts or by replacement of realgar or orpiment by Tl-rich fluids.

Chemical Composition

Two grains of fangite, containing no microscopically visible impurities, were analyzed using a fully automated Cameca SX50 electron microprobe operated at 15 kV and 10 nA. These operating conditions were used to avoid damage to the crystal surfaces and subsequent volatization of elements. The standard used in the analysis was natural lorandite (previously analyzed using other standards for Tl, As, and S). This resulted in the following average analytical values and their ranges: Tl 75.7(8)% (74.6–76.8%), As 9.16(4)% (9.10–9.20%), S 15.6(1)% (15.5–15.8%), and mean total 100.4(8)%. Other elements (Fe, Cu, Zn, Au, Sb, Se, Te, and Ni) were sought, but their concentrations (below 0.2 wt%) were considered insignificant, as they were near the detection limit of the instrument. These values give a formula that is almost exactly the ideal of Tl_3AsS_4.

The composition of the material from Alshar was reported by El Goresy and Pavicevic (1988) as Tl 72.9, As 9.40, and S 15.8%. The elements Sb, Fe, Zn, Cu, and Ni were all below 0.22%, although they noted Sb as being detectable. Their reported values of Tl are slightly lower than ours, leading them to infer a Tl site occupancy of fewer than three atoms. This is not confirmed by our analyses and crystal structure determination.

X-ray powder diffraction data

A Gandolfi pattern of fangite was obtained from a group of approximately 15 crystallites ranging in size from 4–125 μm, but a much higher quality powder pattern was acquired from synthetic Tl_3AsS_4, using an automated powder diffractometer (Table 1). The synthetic material used in the powder diffraction and optical studies was taken from a crystal 1.0 × 1.0 × 2.5 cm, which was kindly supplied by M. Gottlieb of the Westinghouse Research Laboratories, Pittsburgh, Pennsylvania 15235, who synthesized the compound to study its optoacoustic properties (Roland et al., 1972).

Physical properties

Fangite is translucent and has a deep red to maroon color, similar to that of gillulyite and lorandite, which also occur at the Mercur Au deposit. It tarnishes to darker, nearly metallic colors. In bright sunlight the color is distinctively different from the orange-red to red color of realgar. No streak was obtained from natural fangite, but synthetic Tl_3AsS_4 has an orange streak. The luster is vitreous, becoming metallic in appearance as the mineral tarnishes. There was too little of the natural material to determine hardness, but hardness was measured on the synthetic Tl_3AsS_4. Hardness was determined with a Leitz Miniload 2 microhardness tester at a loading of 100 g. Ten indentations were made, yielding a VHN_{100} mean of 60.7 and a range of 59.3–63.3. All of the indentations were slightly fractured with concave margins. The approximate corresponding Mohs hardness is between 2 and 2.5.

The calculated density of fangite is 6.185 g/cm^3; measured density was not determined because of the small size of the grains and the limited material available. The measured density of synthetic Tl_3AsS_4 is 6.20(4) g/cm^3 (Roland et al., 1972).

No well-formed crystals were found. When the vug was opened, the fangite grains exhibited relatively flat surfaces, which may represent cleavage, but no distinctive cleavage was noticeable on the few grains available for study. The synthetic material exhibits conchoidal fracture.

TABLE 1. X-ray powder data for synthetic and natural fangite

Synthetic*				Natural**	
hkl	d_{calc}†	d_{obs}	I/I_o	d_{obs}	I_{est}
002	4.540	4.534	6		
200	4.447	4.438	8	4.43	w
121	4.127	4.119	23	4.14	m
210	4.115				
201	3.994	3.981	58	3.99	s
112	3.789	3.792	34	3.80	m
022	3.482	3.476	34	3.47	m
220	3.440	3.434	32		
031	3.361	3.361	71	3.35	m
122	3.242	3.241	47	3.244	w
221	3.217	3.218	17		
202	3.177	3.174	40		
013	2.915	2.917	23		
103	2.865	2.865	10		
230	2.807	2.807	53	2.813	vs
113	2.770	2.772	18		
222	2.742	2.739	12		
311	2.728	2.726	26	2.731	w
040	2.714	2.714	87		
132	2.696	2.697	14		
231	2.681	2.682	48	2.685	w
123	2.534	2.536	100	2.537	m
213	2.438	2.437	4		
312	2.420	2.417	9		
232	2.387	2.388	4		
223	2.272	2.273	62	2.264	ms
322	2.257	2.256	39		
104	2.199	2.203	8		
410	2.178	2.174	5		
401	2.160	2.159	22	2.162	w
411	2.118				
303	2.118	2.114	25	2.121	vw
051	2.111				
332	2.047	2.049	8		
421	2.007	2.005	12		
152	1.913	1.915	21	1.916	w
251	1.907	1.907	14		
224	1.894	1.895	10		
430	1.894				
134	1.879	1.882	16		
243	1.840	1.840	5		
342	1.832	1.831	5		
105	1.779	1.782	35		
413	1.768				
234	1.765	1.766	8		
053	1.764				
432	1.7483	1.7478	6		
153	1.7303	1.7312	9		
351	1.7199	1.7194	14		
324	1.7104	1.7109	22		
441	1.6899	1.6895	8		
521	1.6618	1.6615	9		
253	1.6397	1.6411	5		
135	1.5965	1.5983	5		
531	1.5722				
262	1.5721	1.5730	12		
414	1.5716				
450	1.5534	1.5531	16		
154	1.5450	1.5463	9		
071	1.5286	1.5294	9		
361	1.5225	1.5225	4		
513	1.5184	1.5175	12		
353	1.5160	1.5159	8		
006	1.5132	1.5123	4		
106	1.4917	1.4906	10		
325	1.4890				
452	1.4697	1.4711	13		
270	1.4642	1.4647	10		
601	1.4630	1.4616	6		
271	1.4456	1.4472	10		
335	1.4236	1.4252	12		
621	1.4125	1.4124	10		
533	1.4119				
504	1.4001	1.4006	8		
461	1.3869	1.3874	10		
354	1.3867				
453	1.3819	1.3822	5		
631	1.3563	1.3563	6		
524	1.3557				
264	1.3482	1.3497	9		
470	1.2719	1.2709	5		
505	1.2707				
174	1.2673	1.2652	4		
553	1.2525	1.2528	8		
535	1.1989	1.1981	5		
643	1.1952	1.1949	16		
382	1.1906	1.1900	6		
742	1.1154	1.1159	6		
733	1.1145				
802	1.0798	1.0797	10		
752	1.0659	1.0648	5		
671	1.0641				
490	1.0602	1.0598	4		
734	1.0600				
457	0.9956	0.9956	5		
209	0.9838	0.9839	6		
851	0.9837				
575	0.9829	0.9828	4		

* The diffraction pattern for synthetic fangite was acquired with a Scintag XDS-2000 APD using a continuous 0.3 °/min scan, Cu$K\alpha$ radiation, 45 kV, 40 mA, a diffracted beam monochromator, and a Si external standard.

** The diffraction pattern for natural fangite was recorded with a 114-mm Gandolfi camera, using a vacuum path, Ni-filtered Cu$K\alpha$ radiation, 45 kV, 12 mA, and a 5.8-h exposure. Approximately 15 crystallites, ranging in size from 4 to 125 μm, were used.

† The unit-cell parameters used to calculate the *d* values were obtained from natural fangite using 25 strong reflections collected on a Rigaku AFC5S four-circle diffractometer (see Table 3). Intensity data from the structural study were used as an aid during indexing.

OPTICAL INVESTIGATIONS

Optical properties of fangite

Polishing and measuring procedures were as outlined in Criddle et al. (1983), except that a silicon carbide reflectance standard (Zeiss no. 472) was used for all measurements. These were made with air and oil objectives (16×), the numerical apertures of which were adjusted to 0.15. The oil used for immersion measurements was Zeiss DIN 58 884 (n_D = 1.515).

Several grains of fangite are exposed in the polished section of the type material, but only one grain was suitable for measurement because of the nearly ubiquitous presence of red internal reflections, which are characteristic of fangite. In the measurement of specular reflectance of translucent minerals, it is essential that internal reflections be avoided; if they are not, the incident beam will be reflected both from the surface and from within the crystal. The result is an incremental error that will vary with wavelength and that, for fangite, would mean that the biggest errors would occur at the red end of the spectrum. See Dunn et al. (1988) for a further discussion of these phenomena.

Fortunately, mounts of both the type specimen and synthetic Tl_3AsS_4 contain grains in which cleavages or

TABLE 2. *R* and ^{im}R data and color values for fangite, its synthetic equivalent, and gillulyite

λ	Fangite		Synthetic		Gillulyite		Fangite		Synthetic		Gillulyite	
(nm)	R_1	R_2	R_1	R_2	R_1	R_2	$^{im}R_1$	$^{im}R_2$	$^{im}R_1$	$^{im}R_2$	$^{im}R_1$	$^{im}R_2$
400	29.1	30.15	28.5	29.5	29.8	32.0	13.8	14.7	13.6	14.7	15.0	18.6
420	28.5	29.5	28.2	29.1	29.3	31.8	13.4	14.3	13.3	14.5	14.6	18.1
440	27.6	28.7	27.8	28.7	28.6	31.55	12.7	13.8	12.7	13.9	13.9	17.7
460	26.8	27.8	27.05	27.95	27.8	31.0	12.1	13.0	12.2	13.3	13.2	17.05
470	26.4	27.35	26.7	27.6	27.3	30.6	11.8	12.6	11.9	12.9	12.7	16.65
480	26.0	26.8	26.3	27.1	27.0	30.4	11.5	12.2	11.6	12.5	12.4	16.25
500	25.2	25.9	25.5	26.1	26.1	29.6	10.9	11.5	11.0	11.8	11.6	15.5
520	24.5	25.0	24.8	25.2	25.1	28.9	10.4	10.8	10.45	11.1	10.9	14.8
540	23.8	24.25	24.0	24.4	24.3	28.2	9.89	10.2	9.94	10.4	10.3	14.1
546	23.65	24.1	23.9	24.2	24.1	28.0	9.77	10.1	9.81	10.3	10.1	13.9
560	23.3	23.6	23.4	23.7	23.6	27.5	9.49	9.81	9.48	9.92	9.76	13.5
580	22.8	23.1	22.8	23.1	23.1	26.9	9.13	9.43	9.10	9.51	9.36	12.9
589	22.5	22.9	22.6	22.9	22.8	26.6	8.99	9.27	8.92	9.35	9.19	12.6
600	22.3	22.7	22.4	22.7	22.6	26.25	8.85	9.14	8.80	9.22	9.03	12.4
620	22.0	22.3	22.1	22.4	22.2	25.8	8.66	8.93	8.54	8.96	8.77	12.0
640	21.7	22.05	21.8	22.0	21.9	25.4	8.49	8.74	8.37	8.76	8.59	11.8
650	21.6	21.95	21.6	21.9	21.7	25.3	8.40	8.65	8.30	8.68	8.47	11.7
660	21.5	21.8	21.5	21.8	21.6	25.2	8.32	8.59	8.20	8.62	8.45	11.6
680	21.3	21.6	21.3	21.5	21.35	24.9	8.19	8.43	8.07	8.47	8.27	11.4
700	21.1	21.5	21.1	21.4	21.2	24.8	8.08	8.34	7.97	8.36	8.14	11.2
					Color values for CIE illuminant C (6,774 K)							
x	0.294	0.292	0.293	0.292	0.292	0.295	0.282	0.279	0.281	0.278	0.277	0.282
y	0.298	0.300	0.300	0.298	0.298	0.303	0.287	0.283	0.287	0.283	0.282	0.290
Y%	23.5	23.9	23.7	24.1	23.9	27.7	9.4	9.7	9.7	10.2	10.0	13.7
λ_d	478	477	478	478	478	480	476	477	478	477	477	478
P_e%	7.9	8.7	8.0	8.9	8.9	6.9	13.4	15.1	13.9	15.4	16.0	13.1

fractures inclined at an angle to the polished surface reflect those unwanted components of the incident beam away. The reflectance data (Table 2) and color values for the synthetic material and the type specimen are in remarkable agreement; they confirm that the mineral has a very low bireflectance, with a difference in Y% of 0.4. As this is very close to the limits of confidence of reflectance measurement, it might be considered that the grains measured were nearly isotropic; however, repeated measurements of both sections (not included in Table 2) proved this 0.4% difference to be reproducible. The monotonous reduction in reflectance from the blue to red end of the visible spectrum is consistent with the blue-gray appearance of fangite in polished section, which, in turn, is in keeping with its appearance in hand specimen (or thin section) as red and translucent. Refractive indices (n) calculated from the R data (using the Koenigsberger equations) reveal a trend from 3.1–3.3 at 400 nm to 2.6–2.7 at 700 nm, with values at 589 nm between 2.78 and 2.80. The corresponding trend within the absorption coefficients (k) is from 0.8–1.1 to <0.1–0.3, with values at 589 nm of 0.26–0.30.

Comparison of these reflectance spectra with those in the Quantitative Data File for ore minerals (Criddle and Stanley, 1986) shows that there are similarities between R_1 and R_2 of fangite and the R_1 values of proustite (Ag_3AsS_3); however, proustite is distinctly bireflectant and, with its somewhat higher reflectances at the blue end of the spectrum, is more purplish red in appearance.

Revision of optical data for gillulyite

Because of the problems with internal refections in fangite, data for a cotype specimen of gillulyite (NMNH 170773) were remeasured, since it was thought likely that the same problem had affected the data previously reported by Wilson et al. (1991). Exactly the same measurement and preparation procedures were followed as for fangite. The data obtained (Table 2) prove an even closer similarity between the R_1 values for gillulyite and the values for the two vibration directions of fangite. Gillulyite is, however, almost identically bireflectant as proustite. In fact, the only way the two minerals could be identified optically as different species is from measurement of the complete visible spectrum, since the dispersion of the reflectance for gillulyite (for both vibration directions) is identical with that of fangite. It follows that the only way one can tell gillulyite and fangite apart optically is on the basis of the much greater bireflectance of the former. It is worth noting that the refractive indices of gillulyite at 589 nm are nearly identical for both vibration directions and correspond closely to those of fangite (n = 2.81). The differences in bireflectance, in this instance, are explained by the contribution from absorption, with absorption coefficients varying from 0.2 to 0.9 at 589 nm. The tabulated reflectance data for gillulyite replace those originally published by Wilson et al. (1991), since it is now apparent that the latter were subject to the effects of internal reflections.

STRUCTURE DETERMINATION AND REFINEMENT

A small quantity of fangite was obtained from the vug described previously. Most of the resulting fragments were unsuitable for single-crystal work. However, after several attempts, a fragment was found that produced reasonably symmetrical peak shapes, if not overwhelming peak intensities. The standard experimental details are given in

Table 3. Experimental details for fangite

Crystal data	
Tl_3AsS_4	$V = 877(1)$ Å^3
$M_r = 816.28$	$Z = 4$
Orthorhombic	$D_x = 6.185$ g/cm^3
Pnma	Mo$K\alpha$
$a = 8.894(8)$ Å	$\lambda = 0.71069$ Å
$b = 10.855(9)$ Å	$\mu = 601.46$ cm^{-1}
$c = 9.079(9)$ Å	$T = 296$ K
Cell parameters from 25 reflections	irregular fragment
$2\theta = 10–23°$	0.15 × 0.14 × 0.08 mm
	red color
Data collection	
Rigaku AFC5S diffractometer	$2\theta_{max} = 60°$
	$h = 0 \rightarrow 12$
Absorption correction:	$k = 0 \rightarrow 15$
Difabs empirical	$l = 0 \rightarrow 12$
$T_{min} = 0.71$, $T_{max} = 1.61$	three standard reflections
Measured reflections: 1342	frequency: 100 ref.
Observed reflections: 637 [$I > 3\sigma(I)$]	intensity variation: 1.4%
Refinement	
Refinement on F	$(\Delta/\sigma)_{max} = 0.0002$
Final $R = 0.046$	$(\Delta\rho)_{max} = 3.04$ e/Å^3
$R_w = 0.045$	$(\Delta\rho)_{min} = -2.85$ e/Å^3
$S = 1.30$	Extinction correction:
Observed reflections: 637	Zachariasen Gaussian
Parameters: 44	Coefficient = 0.30(18) × 10^{-7}
$w = 4F_o^2/\sigma^2(F_o^2)$	

Table 3. A scan speed of 1°/min (in ω) was used and weak reflections [$I < 10.0\sigma(I)$] were rescanned (maximum of two rescans) and the counts accumulated to improve accuracy. The irregular shape of the grain precluded the use of an analytical or numerical absorption correction. The Difabs empirical absorption correction that was utilized (Walker and Stuart, 1983) proved to be superior to the ψ-scan method. The atomic position of Tl1 was found by utilizing the direct-methods program Mithril (Gilmore, 1984), whereas the remaining atomic sites were located by application of the phase expansion, symbolic addition program Dirdif (Beurskens, 1984). Full-matrix, least-squares refinement was performed to minimize $\Sigma w(|F_o| - |F_c|)^2$. Atomic scattering factors and anomalous dispersion corrections were taken from the *International Tables for X-ray Crystallography* (Ibers and Hamilton, 1974). All computer programs were from Texsan (Molecular Structure Corporation, 1985).

Table 4 gives the final refined positional and displacement parameters. Bond distances, average distances, and angles are presented in Table 5. There are no appreciable differences in atomic positions or bond distances between the synthetic and the natural material. Synthetic Tl_3AsS_4 produced a residual of 0.04, as compared with 0.046 for fangite. The observed and calculated structure factors are listed in Table 6.[1]

Table 5. Bond distances (Å) and angles (°) for fangite

As tetrahedron				
As-S3	2.163(7)	S3-S3h	109.9(4)	3.54(2)
As-S3h	2.163(7)	S3-S2g	111.8(2)	3.58(1)
As-S2g	2.165(9)	S3-S1	107.9(2)	3.52(1)
As-S1	2.196(9)	S3h-S2g	111.8(2)	3.58(1)
		S3h-S1	107.9(2)	3.52(1)
		S2g-S1	107.3(4)	3.51(1)
Average	2.172			

Tl1 polyhedron		Tl2 polyhedron	
Tl1-S1	3.100(7)	Tl2-S3e	3.072(7)
Tl1-S1a	3.209(7)	Tl2-S3f	3.072(7)
Tl1-S3	3.222(8)	Tl2-S2e	3.12(1)
Tl1-S3d	3.263(7)	Tl2-S1	3.191(8)
Tl1-S2b	3.278(7)	Tl2-S2b	3.394(9)
Tl1-S3c	3.445(7)		
Tl1-S2c	3.499(4)		
Average	3.288	Average	3.170

Note: symmetry operators are as follows: a = ½ + x, ½ − y, ½ − z; b = x, y, −1 + z; c = −x, −y, 1 − z; d = ½ − x, −y, −½ + z; e = ½ + x, ½ − y, ½ − z; f = ½ + x, y, ½ − z; g = ½ + x, ½ − y, 1½ − z; h = x, ½ − y, z.

The fangite structure

General description

Figure 1 shows the polyhedral arrangement in fangite as viewed down the **a** axis (**a** extends from 0 to ½). The As atom is in nearly perfect tetrahedral coordination with S (average bond length 2.172 Å), whereas the Tl2 atom is in fivefold coordination with S, forming a distorted trigonal dipyramid (average bond length of 3.17 Å); the tetrahedra and the dipyramids are shown as solid polyhedra. The Tl1 atom is in sevenfold coordination with S (average bond length 3.288 Å), forming a distorted, monocapped octahedron (shown in ball and spoke representation). In this view, the structure appears to be composed of chains parallel to the **c** axis. Each chain is composed of alternating Tl2 dipyramids and As tetrahedra, which are interconnected by corner sharing at S1 and S2. The chains are linked in the **b** direction by Tl1 polyhedra, which share edges with neighboring dipyr-

[1] To obtain a copy of Table 6, order Document AM-93-538 from the Business Office, Mineralogical Society of America, 1130 Seventeenth Street NW, Suite 330, Washington, DC 20036, U.S.A. Please remit $5.00 in advance for the microfiche.

Table 4. Atomic coordinates, anisotropic displacement parameters, and B equivalents for fangite

	x	y	z	U_{11}	U_{22}	U_{33}	U_{12}	U_{13}	U_{23}	B_{eq}
Tl1	0.0612(1)	0.0494(1)	0.1958(1)	0.0331(5)	0.0236(5)	0.0314(5)	0.0021(6)	−0.0005(5)	−0.0028(5)	2.32(4)
Tl2	0.3837(2)	¼	−0.1094(2)	0.0249(8)	0.064(1)	0.0280(8)	0	0.0020(7)	0	3.07(8)
As	0.2807(4)	¼	0.4744(4)	0.015(2)	0.020(2)	0.014(2)	0	−0.000(1)	0	1.3(1)
S1	0.306(1)	¼	0.2338(8)	0.021(4)	0.033(5)	0.006(4)	0	−0.001(3)	0	1.6(3)
S2	0.004(1)	¼	0.932(1)	0.020(4)	0.032(6)	0.024(4)	0	0.005(4)	0	2.0(4)
S3	0.1557(7)	0.0869(7)	0.5354(8)	0.028(3)	0.024(4)	0.035(4)	−0.008(3)	0.002(3)	0.006(3)	2.3(3)

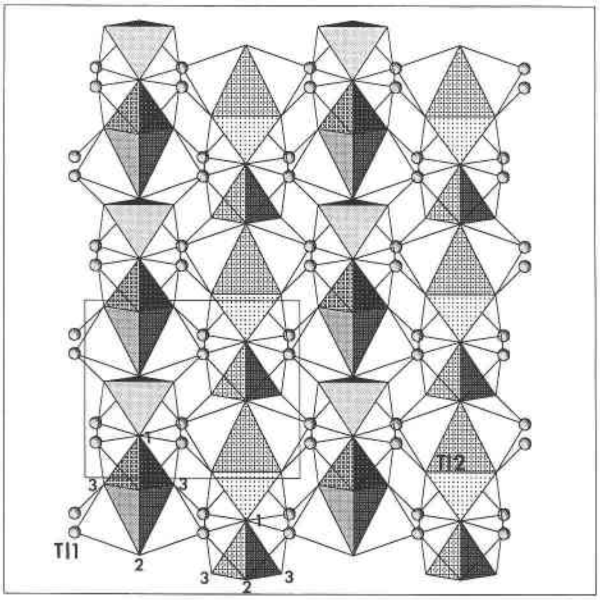

Fig. 1. The polyhedral arrangement in fangite as viewed down the **a** axis. The S atoms are indicated by numbers, e.g., 1 = S1, etc. The inset rectangle shows the unit-cell outline; the **b** axis is horizontal, and the **c** axis is vertical.

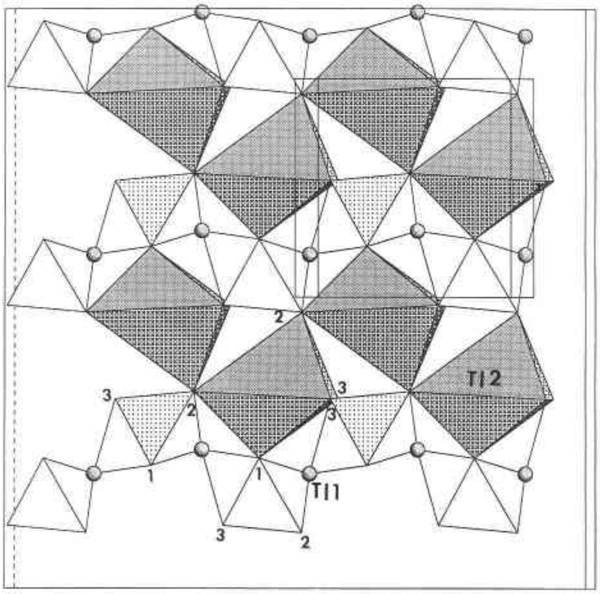

Fig. 2. The layer structure as viewed parallel to the **b** axis. The **a** axis is horizontal and the **c** axis is vertical. The structure has been rotated slightly about the **c** axis.

amids and tetrahedra. The symmetry of the space group causes every other chain to be rotated 180° and moved up and down the **a** axis.

Figure 2 shows an isolated chain as viewed down the **b** axis (**b** extends from 0 to ¼). In this orientation it becomes obvious that the previously described chain is actually a Tl2-As polyhedral layer. The layer is composed of zigzag chains of Tl2 trigonal dipyramids that parallel **a** and are joined in the **c** direction by As tetrahedra. The tetrahedra share one edge and two vertices with the dipyramids to form nearly planar Tl2-As polyhedral layers parallel to (010). The layers are linked in the **b** direction by interlayer Tl1 atoms.

Table 7 presents calculated empirical bond valences for fangite based on bond valence parameters of Brown and Altermatt (1985). The bond valences around Tl, As, and S are within the accepted range of values. The formal valence state of As in fangite is +5, although in most other similar species As is trivalent. Among common sulfosalts, pentavalent As is found only in enargite.

The Tl1 polyhedron

The Tl1 atom forms a highly distorted monocapped octahedron in sevenfold coordination with S atoms. The Tl1-S distances range from 3.100 to 3.499 Å (Table 5). We consider the Tl1-S2 distance of 3.499 Å to be a bond because the corresponding bond valence is 0.08. Brown (1974) suggested that a bond should be considered legitimate if the bond valence is equal to or greater than 0.08. In earlier work on synthetic Tl_3AsS_4 (Engel and Nowacki, 1984), Tl1 was also reported to be in sevenfold coordination. In bernardite, $TlAs_5S_8$, Tl is in eightfold coordination and distances range from 3.05 to 3.563 Å (Pašava et al., 1989). However, two of the bonds, Tl1-S6 and Tl1-S2, are questionable, as the distances 3.563 and 3.544 Å are too long, based on the criterion stated above. In parapierroitite, $TlSb_5S_8$, Engel (1980) reported $^{[8]}$Tl-S and $^{[9]}$Tl-S distance ranges of 3.235–3.695 and 3.126–3.712 Å, respectively. He described the coordination polyhedra as "trigonal prisms with two or three additional atoms located near the side faces." From the bond-valence point of view, we can reject one $^{[8]}$Tl-S and two $^{[9]}$Tl-S distances as being too large. Thus we would consider both Tl atoms to be in sevenfold coordination, and the average distances agree with ours (Table 5). Following similar reasoning, we find sevenfold coordination around Tl in simonite, $TlHgAs_3S_6$ (Engel et al., 1982), and an average Tl-S distance of 3.345 Å. In imhofite, $Tl_{5.6}As_{15}S_{25.3}$ (Divjaković and Nowacki, 1976), Tl2 is in sevenfold coordination, with an average Tl-S distance of 3.37 Å. Divjaković and Nowacki (1976) considered Tl1 to be in eightfold coordi-

Table 7. Bond valences for fangite

	Tl1	Tl2	As*	Total
S1	0.223·2, 0.166·2 0.166	0.174	1.19	2.142
S2	0.138·2, 0.076·2 0.076	0.101, 0.211 0.211	1.29	2.030
S3	0.160, 0.088, 0.144 0.088 0.144	0.241 0.241	1.30 1.30	1.933
Total	0.995	0.968	5.08	

* The r_o for As is 2.26 (I.D. Brown, personal communication).

nation, but, if we omit the supposed Tl1-S6 bond of 3.65 Å, we again obtain sevenfold coordination, with an average Tl-S distance of 3.31 Å.

Unlike in many of the thallium sulfosalts mentioned above, the coordination of Tl in fangite is not concentrated on one side of the atom. The Tl1 atoms link the individual Tl2-As layers through four bonds on one side of Tl1 and three on the other.

The Tl2 polyhedron

The S atoms around Tl2 in fangite form a distorted trigonal dipyramid. The distances of Tl2 from the three equatorial vertices, i.e., from S2, S3e, and S3f, are 3.398, 3.072, and 3.072 Å, respectively, whereas the apical S1 and S2e distances are 3.192 and 3.118 Å, respectively (Table 5). In lorandite, $TlAsS_2$ (Fleet, 1973), Tl1-S, and Tl2-S distances range from 2.96 to 3.69 and 2.97 to 3.89 Å, respectively. However, Fleet (1973) placed an arbitrary limit of 3.40 on Tl-S distances. As a result, Tl1 and Tl2 are both in fivefold coordination, producing polyhedra that were described as flattened square pyramids. In ellisite, Tl_3AsS_3 (Gostojić, 1980), Tl is in fivefold (3 + 2) coordination with S atoms and the average Tl-As distance is 3.216 Å. In synthetic Tl_3AsS_4, Tl2 is also fivefold coordinated, with an average Tl2-S distance of 3.176 Å, in good agreement with the results obtained from fangite.

The As polyhedron

Only one As atom is present in the asymmetric unit, and the coordination with S is tetrahedral. The As-S distances range from 2.163 to 2.196 Å, the average being 2.172 Å (Table 5). Similar coordination of the As atom was observed in synthetic Tl_3AsS_4, with a mean As-S distance of 2.164 Å (Engel and Nowacki, 1984), and in enargite (Adiwidjaja and Löhn, 1970), with a mean As-S distance of 2.18 Å. In luzonite (Marumo and Nowacki, 1967), the average $^{[4]}$As-S distance is 2.26 Å. This rather large value is due to the presence of significant Sb substituting for As.

Acknowledgments

Part of this work was supported by a grant (to J.R.W.) from the Research and Professional Growth Committee, Weber State University. Assistance with microprobe analyses was provided by W.P. Nash and R. Lambert of the University of Utah. J.M. Hughes of University Miami (Ohio) kindly obtained the Gandolfi powder pattern. L. Stanger and other personnel at Barrick Mercur Gold Mines, Inc., have been very helpful in allowing access to the mine and assisting in the collecting of material. C.J. Stanley of the Natural History Museum assisted with the optical determinations. Reviews by E. Foord and R. Rouse were very helpful in correcting the many problems resulting, in part, from the untimely death of one of the authors (P.K.S.G.) during the preparation of the manuscript.

References cited

Adiwidjaja, G., and Löhn, J. (1970) Strukturverfeinerung von Enargit, Cu_3AsS_4. Acta Crystallographica, B26, 1878–1879.

Beurskens, P.T. (1984) DIRDIF: An automatic procedure for phase extension and refinement of difference structure factors. Technical Report 1984/1. University of Nijmegen, The Netherlands.

Brown, I.D. (1974) Bond valence as an aid to understanding the stereochemistry of O and F complexes of Sn(II), Sb(III), Te(IV), I(V) and Xe(VI). Journal of Solid State Chemistry, 11, 214–233.

Brown, I.D., and Altermatt, D. (1985) Bond-valence parameters obtained from a systematic analysis of the inorganic crystal structure database. Acta Crystallographica, B41, 244–247.

Criddle, A.J., and Stanley, C.J., Eds. (1986) The quantitative data file for ore minerals of the Commission on Ore Microscopy of the International Mineralogical Association (2nd edition). British Museum, London.

Criddle, A.J., Stanley, C.J., Chisholm, J.E., and Fejer, E.E. (1983) Henryite, a new copper-silver telluride from Bisbee, Arizona. Bulletin de Minéralogie, 106, 511–517.

Divjaković, V., and Nowacki, W. (1976) Die Kristallstruktur von Imhofit, $Tl_{5.6}As_{15}S_{25.3}$. Zeitschrift für Kristallographie, 144, 323–333.

Dunn, P.J., Peacor, D.R., Criddle, A.J., and Stanley, C.J. (1988) Ingersonite, a new calcium-manganese antimonate related to pyrochlore, from Långban, Sweden. American Mineralogist, 73, 405–412.

El Goresy, A., and Pavicevic, M.K. (1988) A new thallium mineral in the Alshar deposit in Yugoslavia. Die Naturwissenschaften, 75, 37–39.

Engel, P. (1980) Die Kristallstruktur von synthetischem Parapierrotit, $TlSb_5S_8$. Zeitschrift für Kristallographie, 151, 203–216.

Engel, P., and Nowacki, W. (1984) Refinement of the crystal structure of synthetic Tl_3AsS_4. Croatica Chemica Acta, 57, 499–505.

Engel, P., Nowacki, W., Balić-Žunić, T., and Ščavničar, S. (1982) The crystal structure of simonite, $TlHgAs_3S_6$. Zeitschrift für Kristallographie, 161, 159–166.

Fleet, M.E. (1973) The crystal structure and bonding of lorandite, $Tl_2As_2S_4$. Zeitschrift für Kristallographie, 138, 147–160.

Gilluly, J. (1932) Geology and ore deposits of the Stockton and Fairfield Quadrangles, Utah. U.S. Geological Survey Professional Paper, 173, 171 p.

Gilmore, C.J. (1984) MITHRIL: An integrated direct-methods computer program. Journal of Applied Crystallography, 17, 42–46.

Gostojić, M. (1980) Die Kristallstruktur von synthetischem Ellisit, Tl_3AsS_3. Zeitschrift für Kristallographie, 151, 249–254.

Ibers, J.A., and Hamilton, W.C., Eds. (1974) International tables for X-ray crystallography, vol. IV, 366 p. Kynoch, Birmingham, England.

Jewell, P.W., and Parry, W.T. (1987) Geology and hydrothermal alteration of the Mercur gold deposit, Utah. Economic Geology, 82, 1958–1966.

——— (1988) Geochemistry of the Mercur gold deposit (Utah, U.S.A.). Chemical Geology, 69, 245–265.

Kornze, L.D. (1987) Geology of the Mercur gold mine. In J.L. Johnson, Ed., Bulk mineable precious metal deposits of the western United States: Guidebook for field trips, p. 381–389. Geological Society of Nevada, Reno, Nevada.

Kroko, C.T., and Bruhn, R.L. (1992) Structural controls on gold distribution, Mercur gold deposit, Tooele County, Utah. In J.R. Wilson, Ed., Field guide to geologic excursions in Utah and adjacent areas of Nevada, Idaho, and Wyoming, p. 325–332. Miscellaneous Publication 92-3, Utah Geological Survey, Salt Lake City, Utah.

Marumo, F., and Nowacki, W. (1967) A refinement of the crystal structure of luzonite, Cu_3AsS_4. Zeitschrift für Kristallographie, 124, 1–8.

Molecular Structure Corporation (1985) TEXSAN-TEXRAY structure analysis package. The Woodlands, Texas.

Pašava, J., Pertlik, F., Stumpfl, E.F., and Zemann, J. (1989) Bernardite, a new thallium arsenic sulphosalt from Allchar, Macedonia, with a determination of the crystal structure. Mineralogical Magazine, 53, 531–538.

Roland, G.W., Gottlieb, M., and Feichtner, J.D. (1972) Optoacoustic properties of thallium arsenic sulphide, Tl_3AsS_4. Applied Physics Letters, 21, 52–54.

Stanger, L.W. (1992) Barrick Mercur gold mine, Mercur, Utah. In J.R. Wilson, Ed., Miscellaneous publication 92-3: Field guide to geologic excursions in Utah and adjacent areas of Nevada, Idaho, and Wyoming, p. 319–323. Utah Geological Survey, Salt Lake City, Utah.

Tafuri, W.J. (1987) Geology and geochemistry of the Mercur mining district, Tooele County, Utah, 180 p. Ph.D. thesis, University of Utah, Salt Lake City, Utah.

Walker, N., and Stuart D. (1983) An empirical method for correction diffractometer data for absorption effects. Acta Crystallographica, A39, 158–166.

Wilson, P.N., and Parry, W.T. (1990a) Mesozoic hydrothermal alteration associated with gold mineralization in the Mercur district, Utah. Geology, 18, 866–869.

——— (1990b) Geochemistry of Mesozoic hydrothermal alteration of black shales associated with Mercur-type gold deposits. In D.M. Hausen, D.N. Halbe, E.U. Petersen, and W.J. Tafuri, Eds., Gold '90: Proceedings from the Gold '90 Symposium, Salt Lake City, Utah, February 26 to March 1, 1990, p. 167–174. Society of Mining, Metallurgy and Exploration, Littleton, Colorado.

——— (1992) Mesozoic hydrothermal alteration in the Mercur district and surrounding areas: Possible relationships to argillic alteration within the Mercur gold deposits. In J.R. Wilson, Ed., Miscellaneous publication 92-3: Field guide to geologic excursions in Utah and adjacent areas of Nevada, Idaho, and Wyoming, p. 333–341. Utah Geological Survey, Salt Lake City, Utah.

Wilson, J.R., and Wilson, P.N. (1991) Occurrence and paragenesis of thallium sulfosalts and related sulfides at the Barrick Mercur Gold Mine, Utah. In M.L. Allison, Ed., 1990 Guidebook: Energy and mineral resources of Utah, p. 97–112. Utah Geological Society, Salt Lake City, Utah.

——— (1992) Sulfide and sulfosalt mineralogy at the Mercur gold deposit, Tooele County, Utah. In J.R. Wilson, Ed., Miscellaneous publication 92-3: Field guide to geologic excursions in Utah and adjacent areas of Nevada, Idaho, and Wyoming, p. 343–347. Utah Geological Survey, Salt Lake City, Utah.

Wilson, J.R., Robinson, P.D., Wilson, P.N., Stanger, L.W., and Salmon, G.L. (1991) Gillulyite, $Tl_2(As,Sb)_8S_{13}$, a new thallium arsenic sulfosalt from the Mercur gold deposit, Utah. American Mineralogist, 76, 653–656.

Manuscript received October 6, 1992
Manuscript accepted May 18, 1993